Experimental search for anisotropic flux flow resistivity in the *a-b* plane of optimally doped epitaxial thin films of $YBa_2Cu_3O_{7-\delta}$

G. Koren,* P. Aronov, and E. Polturak
Department of Physics, Technion–Israel Institute of Technology, Haifa 32000, Israel
(Received 28 August 2005; revised manuscript received 17 October 2005; published 6 December 2005)

Transport measurements along the node and antinode directions in the *a-b* plane of optimally doped and epitaxial thin films of $YBa_2Cu_3O_{7-\delta}$ (YBCO) are reported. Low bias magnetoresistance measurements near and below T_c show that the flux flow resistivity along the node and antinode directions vs magnetic field are indistinguishable. This result suggests that within the experimental error of our measurements, *no* correspondence is found between the flux pinning properties in YBCO and the *d*-wave nature of the order parameter.

DOI: 10.1103/PhysRevB.72.212503 PACS number(s): 74.25.Qt, 74.72.Bk, 74.50.+r

Under the applied magnetic field, the apparent resistance of type II superconductors in the mixed state is due to the motion of vortices. In the presence of the transport current, the Lorentz (or Magnus) force on vortices causes motion and induces a voltage drop across the superconducting sample. The ratio of the induced voltage divided by the current defines the flux flow resistance.[1,2] In the Bardeen-Stephen model,[3] valid for the case of weak pinning as, for instance, near T_c, the effective viscosity associated with the motion of vortices is caused by the interaction of the transport current and the shielding currents around the vortex. In the cuprates, the shielding currents around an isolated vortex are predicted to show anisotropy linked to the *d*-wave nature of the order parameter.[4,5] Under the quasiclassical approximation and by the use of the Eilenberger equations, Ichioka *et al.* found a small fourfold anisotropy of a few percent in the induced supercurrents around the vortex core.[4] A preliminary microscopic calculation of vortex tunneling also seems to yield an *anisotropic* vortex dynamics.[5] Although no pinning properties were discussed in these studies, it is still plausible to assume that the effective viscosity which determines the flux flow resistivity may also be anisotropic. The search for this effect is the subject of the present study. We designed a specific, high precision experiment to look for it by magnetotransport measurements which were conducted on nominally identical thin film microbridges of $YBa_2Cu_3O_{7-\delta}$ (YBCO) patterned on the same wafer along the node and antinode directions of the *d*-wave order parameter. We found that the flux flow resistance at low bias did not reveal any anisotropy at the 1% level, which is the stated precision of our measurements.

To facilitate the comparison between the transport properties along the node and antinode directions, two high quality *c*-axis oriented epitaxial thin films of YBCO were prepared under identical conditions by laser ablation deposition on (100) $SrTiO_3$ (STO) wafers of 10×10 mm^2 area. In one case, the orientation of the single crystal STO substrate was with the edge of the wafer parallel to the (010) crystalline direction, while in the other case it was parallel to the (110) direction. Ten microbridges were defined on each wafer using the same photolithographic mask, and patterned by Ar ion milling at a temperature of −170 °C. The dimensions of the microbridges were $0.12\times12\times100$ μm^3. Successive microbridges were oriented at alternating angles of 0° and 45° to the edge of the wafers, so that the transport current would flow either along the node or the antinode of the order parameter. The alternating direction of *adjacent* microbridges was important to minimize systematic differences due to possible inhomogeneities in the films. On the first wafer with the side parallel to the (010) orientation, five odd number bridges were along the antinode direction, and five even number bridges along the node direction. In the second wafer with the side parallel to the (110) orientation, the role of the antinode and node bridges was reversed due to the epitaxial growth of the film. Studying these two types of wafers was done in order to check if our ion milling process, done at an incident angle of 45° to the wafers, is affecting the properties of the microbridges. We note that on the first wafer, the Ar ions milling process leads to antinode bridges with sides normal to the surface, but at an oblique angle for the node microbridges. This situation is reversed in the second wafer. Any observed difference in the transport properties of the two wafers would imply that the effect is not intrinsic, and results from the patterning process. Low resistance gold contacts were prepared on the two wafers by laser ablation deposition and lift off, followed by further oxygen annealing for the gold/YBCO contact (at 650 °C) and the YBCO films themselves (at 450 °C). Transport measurements were done by the standard four-probe dc technique, with and without a magnetic field of up to 8 T normal to the wafers (parallel to the *c* axis).

Figures 1 and 2 show mean values of the zero field normal state resistivity ρ and critical current density J_c on the two wafers, as a function of temperature. The mean values were obtained for each wafer by averaging over three microbridges of each type (node or antinode) which had the closest $T_c(R=0)$ values. The critical current data were measured using a 1 μV per 100 μm bridge length criterion. The normal state resistivities along the node and antinode directions are slightly different, by about 2%. In Fig. 1 the node resistivity is higher, and in Fig. 2 the opposite situation is found where the antinode resistivity is higher. This behavior results from the fact that the ion milling process slightly damages the side of the bridges which are exposed to the Ar ion beam, the node bridges in Fig. 1 and the antinode bridges of Fig. 2. Apart from this minor difference, ρ(node) should be equal to

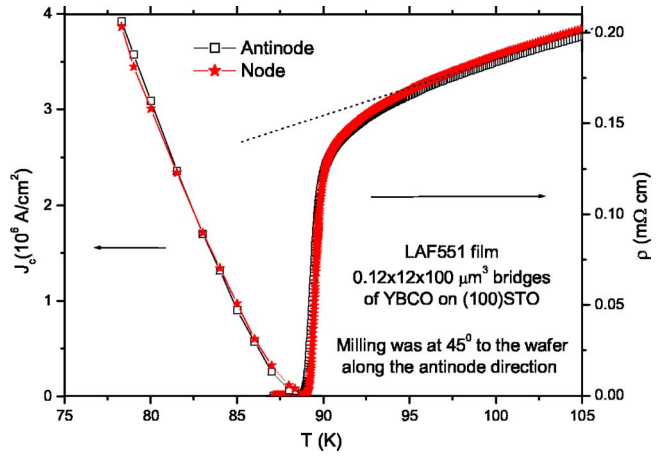

FIG. 1. (Color online) Mean resistivity and critical current density vs temperature of three microbridges of YBCO along an antinode direction (squares), and three along a node direction (stars). The antinode bridges are parallel to the (100) side of the STO wafer, and the node bridges are oriented at 45°. The lines connecting the data points are a guide to the eyes. The straight dashed line extrapolating the normal state resistivity to lower temperatures shows that T_c(onset) is ~94 K.

ρ(antinode) since our films are heavily twinned. This results from the fact that due to twinning, one has $\rho=(\rho_a+\rho_b)/2$ for the antinode bridges, and $\rho=\rho_a\cos^2(45°)+\rho_b\sin^2(45°)$ for the node bridges, which are, of course, equal. The transition temperatures T_c(onset) in Figs. 1 and 2 are identical for both type of bridges. T_c(onset) ~ 94 K is the temperature at which the resistivity data in Figs. 1 and 2 deviates from the straight dashed line extrapolating the high temperature data to lower temperatures. The transition temperatures of zero resistance $T_c(R=0)$ of the node and antinode bridges are very close. In Fig. 1 the values are 88.9 K for the antinode bridges and 89.1 K for the node ones, while in Fig. 2 the corresponding

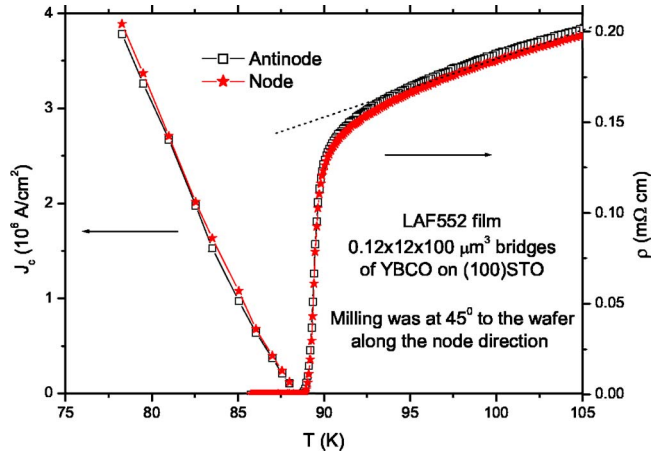

FIG. 2. (Color online) Mean resistivity and critical current density vs temperature of three microbridges of YBCO along an antinode direction (squares), and three along a node direction (stars). The node bridges are parallel to the (110) side of the STO wafer, and the antinode bridges are oriented at 45°. The lines connecting the data points are a guide to the eyes.

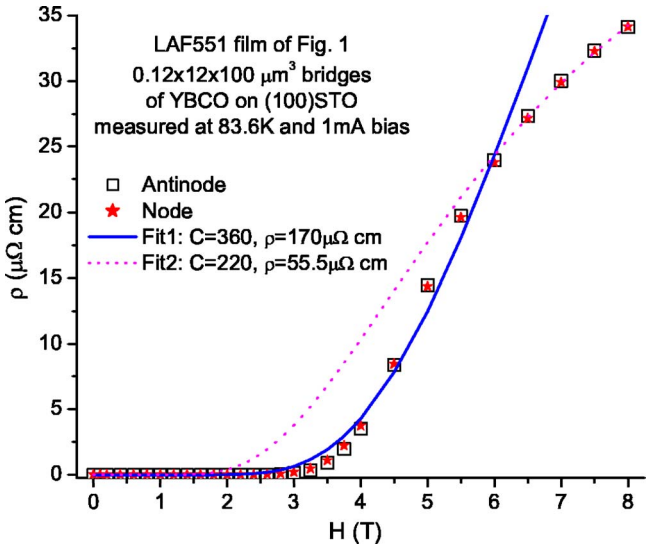

FIG. 3. (Color online) Mean flux flow resistivity at 83.6 K vs applied magnetic field of the bridges of Fig. 1. The mean values are of three bridges along the node direction (stars), and three along the antinode direction (squares). The two curves are fits using the Tinkham's model as given in Eq. (1).

values are 88.8 K and 88.9 K. Although within the experimental noise, the slightly higher T_c by about 0.1% of the node microbridges as compared to the antinode ones, is consistent with Ichioka *et al.* results where the supercurrent around a vortex is slightly higher along the node directions.[4] The differences between the node and antinode bridges are also very small in the critical current results, where near T_c the small difference in T_c affects the results, but at lower temperatures this difference is within the experimental noise. For temperatures close to $T_c(R=0)$, $J_c(T)$ increases with decreasing temperature as $(T_c-T)^{3/2}$, and linearly at lower temperatures with a slope of 0.45×10^6 A/cm^2 K. So we can conclude from Figs. 1 and 2 that the node and antinode bridges have almost identical T_c and $J_c(T)$.

Figures 3 and 4 show the flux flow resistivity of microbridges of Figs. 1 and 2, respectively, as a function of applied magnetic field normal to the wafers. The onset field at which the flux flow resistivity first appears increases with decreasing temperature, due to the stronger pinning of vortices at lower temperatures. Figures 3 and 4 show that the flux flow resistivity curves vs field of both kinds of microbridges, those along the node and antinode directions are almost indistinguishable. This is the main experimental observation of the present study. Both figures also show that at high fields the flux flow resistivity tends to saturate, more so in Fig. 4 than in Fig. 3 due to the higher temperature. This is possibly due to a cross over to the normal state resistivity, although the measured value just above the transition $\rho_N(95\text{ K})=170\ \mu\Omega$ cm (see Figs. 1 and 2) is much higher than the 40–50 $\mu\Omega$ cm value which can be extrapolated from Figs. 3 and 4. The overall behavior of ρ vs H is consistent with the previous experiments on YBCO.[6,7] From the linear part of the data with the highest slope, one can extract the critical field H_{c2} by using the Bardeen-Stephen model.[2,3,6,7] The curves in Figs. 3 and 4 are two Ambegaokar-Halperin type fits using Tinkham's model[8,9] which yields

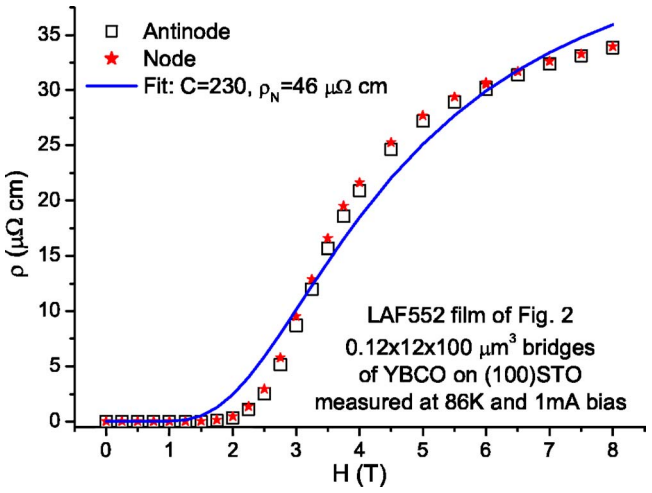

FIG. 4. (Color online) Mean flux flow resistivity at 86 K vs applied magnetic field of the bridges of Fig. 2. The mean values are of two bridges along the node direction (stars), and two along the antinode direction (squares). Mean values were taken here over two and not three microbridges due to contact problems with one of the bridges. The curve is a fit using the Tinkham's model as given in Eq. (1).

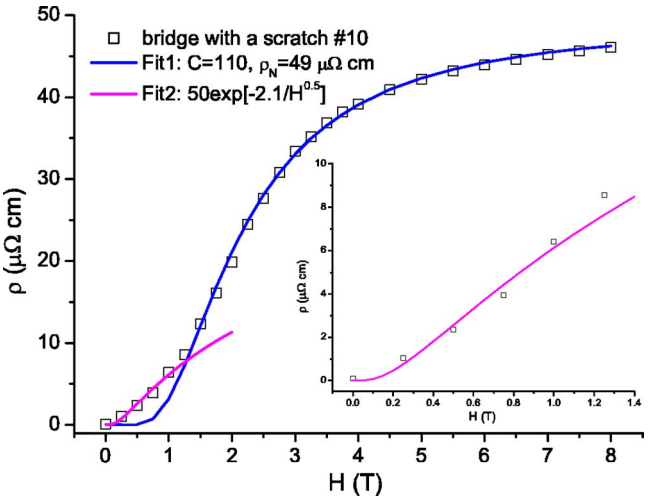

FIG. 5. (Color online) Main panel: Flux flow resistivity of an antinode bridge with a weak link (a scratch) on LAF552 vs applied magnetic field. The curves are fits to the experimental data. Fit1 is obtained by using the Tinkham's model in Eq. (1), and Fit2 is achieved by the tunneling model of Eq. (2). Inset: zoom up on the low-field regime with the tunneling model fit.

$$\rho_{ff} = \rho_N[I_0(U_0/2k_BT)]^{-2} = \rho_N\{I_0[C(1-t)^{3/2}/H]\}^{-2}, \quad (1)$$

where ρ_{ff} and ρ_N are the flux flow and normal state resistivities, I_0 is the modified Bessel function, U_0 is the activation energy, $t=T/T_c$ is the reduced temperature, and C is a constant. The basic physics behind this model is that the motion of vortices between pinning sites is thermally activated and involves phase slippage of 2π like in a single heavily damped current driven Josephson junction. One sees that the fits cannot reproduce the main features of the data all at once. In Fig. 3, we chose to show that they can either fit the data reasonably well up to a field of 6 T but miss the higher fields data (solid curve), or fit the higher fields but miss the onset and the intermediate fields data (dashed curve). In Fig. 4 we chose to show a single fit for the whole range of fields, but then the fit quality is quite poor. We note that the low fields fit in Fig. 3 (Fit 1) is obtained with the actually measured normal state resistivity just above T_c(onset) at 95 K (170 $\mu\Omega$ cm). We shall discuss the reliability and suitability of the Tinkham model later on, here we point out that the important thing is that the model allows us to obtain the activation energy U_0 which is related to the fit parameter C by $U_0=2k_BT_ct(1-t)^{3/2}C/H$ as seen in Eq. (1). Since the node and antinode curves in Figs. 3 and 4, respectively, are almost identical, the same U_0 is obtained for both orientations for each temperature. Therefore, at any given temperature, the activation energy for moving vortices along both directions is the same. This is the main result of the present study. It indicates that the pinning properties of YBCO which control the flux flow resistivity are fully isotropic to within the experimental error, and are not affected by the intrinsic anisotropy of the d-wave order parameter as might be expected.

Finally, we discuss the suitability of using the Tinkham model given in Eq. (1) for the present results. We have already seen the problems involved in using this model in the fits of Figs. 3 and 4. To elucidate this issue, we show in Fig. 5 the flux flow resistivity data vs magnetic field of a microbridge on LAF552 with a weak link in it (a scratch). The weak link leads to a very small critical current in this bridge, and the onset of the flux flow resistivity occurs at a very small field. The solid curve is a fit of this data using Eq. (1). One can see that in this bridge the Tinkham model of a vortex motion by thermal activation fits the data quite nicely except for fields below about 1.5 T. In this regime a different mechanism must be involved in the resistivity behavior vs field and we propose tunneling of vortices as a plausible explanation for the observed result. The standard tunneling probability for crossing a potential barrier of height V and width d is proportional to $\exp[-k\sqrt{Vd}]$, where k is a constant. In the present case, the barrier height is given by the activation energy of the vortex U_0, and the barrier width by the distance between adjacent pinning centers. We take an Anderson-Kim-type activation energy given by Yeshurun and Malozemoff $U_0 \propto 1/H$ [see Eq. (1)],[8,10] and assume a constant tunneling distance between adjacent pinning centers in the weak link as this depends on the specific material properties and not on the magnetic field. This yields a flux flow tunneling current which is proportional to the flux flow resistivity, that for any given temperature is given by

$$\rho_t = A\exp[-D/\sqrt{H}], \quad (2)$$

where A and D are constants. A fit of the data in Fig. 5 up to 2 T using Eq. (2) is shown in this figure and its inset. A reasonably good fit is now obtained for the low-field regime, with a cross over to the Tinkham's model at higher fields. It therefore seems that the Tinkham model is appropriate for films with weak links or defects, but not in the low fields regime. For instance, we could fit the data of Kunchur *et al.*[7] who used films with many defects and weak links reasonably

well, but again, not in the low-field regime where vortex tunneling apparently takes place (similarly to the corresponding fit in Fig. 5). We note that the original Ambegaokar and Halperin model,[9] which was used by Tinkham in his model, was derived for a Josephson junction or a weak link. Tinkham therefore describes his model as a "plausible semiquantitative model" for the dependence of the resistive transition on temperature and magnetic fields. It is thus not surprising that better fits are obtained when weak links are involved. Clearly, the results of Figs. 3 and 4, which were obtained on high quality epitaxial thin films with no weak links, agree with the Tinkham model to a much lesser extent. One can therefore conclude that either this model has to be refined in order to describe our data, or that other effects are involved.

In conclusion, at temperatures close to T_c, low bias and within the experimental error of our measurements, a clear flux flow resistivity isotropy was observed in the present study for the node and antinode directions in the *a*-*b* plane of thin YBCO films. It is therefore demonstrated that the anisotropic *d*-wave nature of the order parameter in YBCO does not induce any measurable anisotropy in the flux pinning properties of the films. We also show that the Ambegaokar and Halperin type model used by Tinkham is more successful in films with weak links.

We are grateful to Rudolf P. Huebener, Guy Deutscher, Assa Auerbach, and Lior Shkedy for useful discussions. This research was supported in part by the Israel Science Foundation (Grant No. 1565/04), the Heinrich Hertz Minerva Center for HTSC, the Karl Stoll Chair in Advanced Materials, and the Fund for the Promotion of Research at the Technion.

*Electronic address: gkoren@physics.technion.ac.il

[1] R. P. Huebener, *Magnetic Flux Structures in Superconductors*, 2nd ed. (Springer-Verlag, Berlin, 2001).
[2] M. Tinkham, *Introduction to Superconductivity*, 2nd ed. (McGraw-Hill, New York, 1996).
[3] J. Bardeen and M. J. Stephen, Phys. Rev. **140**, A1197 (1965).
[4] M. Ichioka, N. Hayashi, N. Enomoto, and K. Machida, Phys. Rev. B **53**, 15316 (1996).
[5] Ari Mizel, cond-mat/0107530 (unpublished).
[6] J. G. Ossandon, J. R. Thompson, D. K. Christen, B. C. Sales, H. R. Kerchner, J. O. Thomson, Y. R. Sun, K. W. Lay, and J. E. Tkaczyk, Phys. Rev. B **45**, 12534 (1992).
[7] M. N. Kunchur, D. K. Christen, and J. M. Phillips, Phys. Rev. Lett. **70**, 998 (1993).
[8] M. Tinkham, Phys. Rev. Lett. **61**, 1658 (1988).
[9] V. Ambegaokar and B. I. Halperin, Phys. Rev. Lett. **22**, 1364 (1969).
[10] Y. Yeshurun and A. P. Malozemoff, Phys. Rev. Lett. **60**, 2202 (1988).